IEEE Access
Multidisciplinary | Rapid Review | Open Access Journal

Received August 18, 2019, accepted September 3, 2019, date of publication September 10, 2019,
date of current version September 25, 2019.

Digital Object Identifier 10.1109/ACCESS.2019.2940294

Reliability Assessment of Distribution Network and Electric Vehicle Considering Quasi-Dynamic Traffic Flow and Vehicle-to-Grid

QIAN ZHANG[1], (Member, IEEE), YI ZHU[1], ZHONG WANG[2], YAOJIA SU[1], AND CHUNYAN LI[1], (Member, IEEE)

[1]State Key Laboratory of Power Transmission Equipment and System Security and New Technology, Chongqing University, Chongqing 400044, China
[2]State Grid Chengdu Power Supply Company, Sichuan 610041, China

Corresponding author: Qian Zhang (zhangqian@cqu.edu.cn)

This work was supported by the National Natural Science Foundation of China under Grant 51507022.

ABSTRACT With the increasing number of electric vehicles and the emergence of vehicle-to-grid technology, electric vehicles have become distributed loads and power sources with random movement characteristics in the distribution network. In order to evaluate the reliability of the distribution network incorporating electric vehicles, firstly, this paper uses the trip chain theory to describe the travel of electric vehicles. Based on the static traffic flow distribution, a high efficiency quasi-dynamic travel simulation method is proposed to consider the influence of traffic congestion on the path selection. Then, the simulation time advancement of the Monte Carlo method is improved, which makes the reliability assessment of the distribution network containing a large amount of electric vehicles' charging and discharging behaviors realizable. Finally, the practicality of the method is verified by the modified IEEE-RBTS Bus-6 test system. The effects of electric vehicles penetration, discharging threshold, and battery capacity on reliability of both distribution networks and electric vehicles are studied.

INDEX TERMS Electric vehicles, reliability, quasi-dynamic travel, Monte Carlo method.

I. INTRODUCTION

In recent years, environmental and energy problems have become increasingly severe. Electric vehicles (EVs) with environmental protection and energy-saving advantages have been proved effective to alleviate energy shortage, environmental pollution and global warming [1]. Electric vehicles have already found scale markets in Japan [2], Europe [3], China [4] and other regions. Under the situation of Energy Internet, energy is flow flexibly for transmission and can be transported to every energy user via electric vehicles [5]. At the same time, the increasing number of EVs becomes a common challenge to maintain the operation of microgrid, which attracts people's attention [6].

As backup power source, electric vehicles can supply power to the grid when a distribution network fails to improve the reliability [7]–[9]. Nowadays, many researches have focused on the reliability assessment of distribution networks with electric vehicles, where analytical methods and simulation methods are used primarily. In [10], an analytical method is proposed to investigate the large scale integration impact of EVs on the grid reliability. Another analytical approach is proposed in [11], through which the reliability impacts of electric vehicles under battery-exchange mode in the distribution level can be assessed. With the improved minimal path method, reliability indices are calculated for various vehicle-to-grid (V2G) and grid-to-vehicle (G2V) to estimate the impact of different level of power exchange on system reliability [12]. Computational efficiency and calculation accuracy are the advantage of the analytic method. However, the electric vehicles have the characteristic of random movement, it is difficult to use the analytical method to calculate its random spatiotemporal state. Based on the statistical modeling method, the V2G-G2V model and time-varying load model of electric vehicles under different control patterns are established in [13], and the sequential Monte Carlo method is used to access the reliability of the distribution system. In [14], V2G and vehicle-to-home (V2H) technologies are used to supply power in the case of power failure with island mode operation. The sequential

The associate editor coordinating the review of this manuscript and approving it for publication was Baoping Cai.

Monte Carlo method is adopted to evaluate the network reliability. However, the literatures above ignore the spatial distribution characteristics of electric vehicles, and there is no research on the relationship between power system and transportation system.

In order to take into account of the mutual coupling relationship between the two systems and maintain a good calculation speed, Ref. [15] uses the vertical coordinate system to represent the road network, and cooperates with the sampling of the travel location to complete the spatial distribution simulation of the electric vehicles. The Monte Carlo simulation method is employed to calculate the reliability index. Although the Cartesian coordinate method can maintain a good calculation speed, the model is too simplified for the road network to consider the impact of traffic congestions on the path simulation.

In the field of intelligent transportation, the static path simulation deems that the traffic congestion of the road section does not change with time. As a result, the simulation accuracy is poor. Meanwhile, the dynamic path simulation takes the real-time changing traffic congestion into consideration. Methods in [16] and software provided by [17] are mature ways for dynamic driving simulation. However, the reliability assessment of the distribution network is to be simulated for decades or even hundreds of years, the calculation of the existing dynamic traffic flow allocation method requires a large amount of calculation time, such techniques are unduly inefficient for reliability assessment. Thus, this paper aims to solve the contradiction between path simulation accuracy and calculation speed and proposes a quasi-dynamic traffic distribution method.

In addition, since a large number of electric vehicles are connected to the grid as load and backup power, their status changes at any time and any place. The simulation time of the traditional Monte Carlo method is no longer applicable at equal intervals, because the time interval should set as short as possible to timely update the status of each electric vehicle, which contains a large amount of invalid calculation when electric vehicles' status stay unchanged. To speed up the Monte Carlo simulation, this paper simulates a single electric vehicle as a unit in which the simulation time advances directly to the start time of the next activity.

In this paper, we establish an assessment method for the reliability of distribution network and electric vehicles, in which traffic simulation and Monte Carlo simulation are improved. First, the trip chain theory is used to describe the travel of electric vehicles. On the basis of static traffic flow distribution, the temporal and spatial distribution and real-time state of charge (SOC) of EVs are obtained by efficient quasi-dynamic simulation method. Based on the former, the influence of electric vehicles penetration, discharge threshold and battery capacity on distribution network and electric vehicles' reliability is studied.

The rest of this paper is organized as follows: Temporal-spatial distribution of EVs based on quasi-dynamic traffic flow model is proposed in Section II. Charging and discharging model of EVs is proposed in Section III. Distribution network reliability assessment is proposed in Section IV. Numerical studies are demonstrated in Section V and conclusions are drawn in Section VI.

II. TEMPORAL-SPATIAL DISTRIBUTION OF EV BASED ON QUASI-DYNAMIC TRAFFIC FLOW MODEL

A. THE TRIP CHAIN OF EVS

This paper focuses on the modeling and analysis of private electric vehicles for the reason they are principle members in V2G [13]. The trip chain model can well describe the driving path of private electric vehicles [18]. Travel destinations can be classified into five types: Home (H), Work (W), Shopping and Eating (SE), Social and Recreational (SR), and Other family/personal errands (O). Based on the travel demands of working days and non-working days, this article divides the trip chain into the following four categories, as shown in Table 1.

TABLE 1. Trip chain ratio of private cars on working days.

Date	No.	Trip chain	Ratio
working days	C_1	H→W→H	p_1
	C_2	H→W→SR/SE/O→H	p_2
non-working days	C_3	H→SR/SE/O→H(a.m.)	p_3
	C_4	H→SR/SE/O→H(p.m.)	p_4

Electric vehicles start in the morning and return home at night on working days. The origin and destination point are fixed, but the trip in the middle is random. Therefore, each vehicle trip chain C can be regarded as probability distribution formula as follows:

$$\begin{aligned} P(C) &= p_i \\ s.t. p_1 + p_2 &= 1 \\ p_3 + p_4 &= 1 \end{aligned} \tag{1}$$

where p_i represents the proportion of each trip chain to the total trip. The proportion of trip chain can be obtained from NHTS survey [19].

Each trip chain consists of a number of trip segments c_{ij}. Take the trip chain C_1 as an example:

$$\begin{cases} C_1 = c_{11} + c_{12} \\ c_{11} = H \rightarrow w \\ c_{12} = W \rightarrow H \end{cases} \tag{2}$$

where the subscript i denotes the trip chain number, j denotes the number of trip segments under the trip chain.

The start time t_s of each trip segment c obeys normal probability distribution [20], and its probability density function is shown in formula (3):

$$f(t_s) = \frac{1}{\sqrt{2\pi}\sigma} \exp\left[-\frac{(t_s-\mu)^2}{2\sigma^2}\right] \tag{3}$$

where μ and σ are the mean and variance of travel time, respectively. Different trip segments correspond to different values.

For (1) and (3), the type of trip chain and departure time can be extracted by Monte Carlo simulation.

B. QUASI-DYNAMIC TRAFFIC FLOW MODEL

In the field of intelligent transportation, there are two simulate methods: static traffic flow simulation And dynamic traffic flow simulation. Static simulation holds that traffic congestion on road sections does not change with time, and the simulation accuracy is poor. Dynamic simulation takes into account the real-time changing traffic conditions, but in order to pursue the accuracy of simulation, the numerical iteration process is very complicated, and the calculation amount is unacceptable.

Inspired by the dynamic driving simulation calculations, this paper divides the time interval on the static incremental path simulation method and then distributes the traffic flow to obtain the time-varying path simulation. Since the time is divided into discrete time intervals, this method is called quasi-dynamic traffic flow Simulatio.

1) OD MATRIX AND TRAFFIC IMPEDANCE

The traffic distribution is usually represented by the OD matrix which describes the number of trips in the investigate area. The electric vehicles included in the same trip segment c_{ij} are counted into the same OD matrix, i.e. one type of trip segment corresponds to an OD matrix, which is called the ''trip segment'' OD matrix, denoted as OD^{ij}. The sum of all trip segment OD matrices is called the total OD travel matrix:

$$\sum_{i}^{q}\sum_{j}^{p} OD^{ij} = OD^{A} \tag{4}$$

where p represents the number of trip segments under the trip chain, q represents the number of trip segments and OD^A represents total travel matrix.

Traffic impedance is usually measured by time. The road travel time function widely used by the Bureau Public Road (BPR) is called the BPR function [21]:

$$t_a = t_0\left[1 + \alpha(\frac{q_a}{c_a})^{\beta}\right] \tag{5}$$

where t_a is the impedance on segment a, t_0 is the zero-current impedance. q_a is the traffic volume on segment a. c_a is the actual capacity of segment a, that is, the number of vehicles that can actually pass through the road in unit time. α and β are the blocking coefficients.

2) STATIC INCREMENTAL ALLOCATION

The static incremental allocation method is an essentially incremental allocation of the shortest path, the detailed steps are as follows:

Step 0: Divide the OD matrix into N layers, set $k = 1$, $x_a^0 = 0$, x_a denotes the traffic volume of the OD matrix allocated to the road segment a.

Step 1: Calculate impedance of each segment, $t_a^k = t_a(x_a^{k-1})$.

Step 2: The shortest path allocation method is used to allocate the k-th layer traffic volume of each OD point pair to the shortest path between them, set as w_a.

Step 3: Accumulate the traffic volume newly allocated for each road segment from step 2 : $x_a^k = x_a^{k-1} + w_a^k$.

Step 4: Stop calculating if $k = N$, otherwise, set $k = k+1$, and return to step 1.

3) QUASI-DYNAMIC PATH SIMULATION METHOD

The static incremental allocation method does not consider the change of road resistance with time and the withdrawal process of EVs from the road network. To solve the problems and maintain a good computational efficiency, this paper proposes a quasi-dynamic traffic distribution method.

a: PERIODIZATION OF OD MATRIX

The departure time of the electric vehicles described above obey the normal distribution shown in formula (3). Each trip segment OD matrix corresponds to a normal distribution curve of the corresponding departure time. We divide a day into N shares. The time interval (hour) can be expressed as:

$$period = \frac{24}{N} \tag{6}$$

Fig. 1 shows the departure time probability density curve corresponding to a trip segment OD matrix, which is divided into N shares in one day:

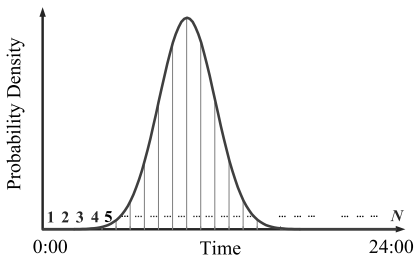

FIGURE 1. OD matrix departure time probability density curve.

Assuming that the traffic impedance in each time interval does not change. During each time interval period, part of the cars in each segment OD matrix will enter the road network. This section is marked as OD_k^{ij}, k denotes the time period number. If the extracted departure time falls in the k-th period, the electric vehicle belongs to OD_k^{ij}, and satisfy:

$$OD^{ij} = \sum_{k=1}^{N} OD_k^{ij} \tag{7}$$

All OD matrices for the k-th period are added to OD_k^A, which is called the period OD matrix:

$$OD_k^A = \sum_{i}^{q}\sum_{j}^{p} OD_k^{ij} \tag{8}$$

$$\sum_{k=1}^{N} OD_k^A = OD^A \tag{9}$$

That is, *ODA* k represents all cars that start in the k-th period.

b: ALLOCATION OF OD MATRIX

This paper assumes that the EVs enter the road network 2 hours before will completely withdraw from the road network. A layer of *OD* matrix will add and a layer of *OD* matrix will exit in each time interval. The traffic volume in i-period can be expressed as:

$$q_a^i = x_a + q_a^{i-1} - q_a^{i-\frac{2}{period}} \tag{10}$$

Corresponding to the road resistance of each time interval, the driving speed of each road section can be obtained by (5) based on departure time and path simulation results. Then temporal-spatial distribution of electric vehicles can be obtained, and the SOC of each electric vehicle at each moment can be calculated. And then based on temporal-spatial distribution of electric vehicles, distribution network reliability could be assessed.

III. CHARGING AND DISCHARGING CIRCUMSTANCE SETTINGS OF EV

A. CHARGING AND DISCHARGING PROBABILITY

The electric vehicles are divided into six types as shown in TABLE 2.

TABLE 2. Types of electric vehicles.

Type	Slow charge at home	Slow charge at workplace
A	Full	Part
B	Full	None
C	Part	Part
D	Part	None
E	None	Part
F	None	None

"Full" means that the owner owns charging equipment, which can fully meet the charging requirements. "Part" means that there are common slow charging piles in the place of residence or workplace, but there is a probability of being occupied by other vehicles, and fast charging is required. "None" means no slow charging devices, only fast mode available. The probability of slow charging p_a is defined to indicate the probability of charging when slow charging is required.

If the electric vehicle is the "Part" type in parking place, there is a probability p_a that it is connected to the grid.

B. CHARGING BEHAVIOR

1) WHEN THE DISTRIBUTION NETWORK IS OPERATING NORMALLY

When electric vehicle i reaches the place of residence or workplace, if the state of charge satisfy formula (11) and the slow charging pile is not occupied, the electric vehicle will be charged with slow mode:

$$SOC_i < \frac{1.5 \cdot E_i^{max}}{E_i^{all}} \cdot 100\% = S_i \tag{11}$$

where S_i is the charging threshold of vehicle i, SOC_i is the state of charge; E_i^{all} is the battery capacity; E_i^{max} represents the maximum of daily power consumption. A scaling factor of 1.5 is set to prevent the car from running out of power on the road caused by emergencies.

If the battery is fully charged before the next travel, the charging duration can be expressed as (12):

$$T_c = \frac{E_i^{all} - E_i}{P_c^{slow}} \tag{12}$$

where T_c is the charging duration, P_c^{slow} is the slow charging power.

If the electric vehicle is not fully charged before the next trip, the charging duration is expressed as (13), and the battery power can be presented as (14):

$$T_c = T_l - T_s \tag{13}$$

$$E_i^l = E_i^s + P_c^{slow} \cdot T_c \tag{14}$$

where T_l represents the departure time, T_s represents the start time of charging, E^l represents the battery level of the electric vehicle at the moment of departure, and E^s represents the battery level at the start of charging.

If the electric vehicle should be charged with slow mode, but the charging pile is occupied, it has to be charged with fast mode before next trip. If there are multiple fast charging stations in the travel path, one of them is randomly selected for energy supplement. If there is no charging station in the travel path, the fast charging station closest to the starting point is selected for charging. The battery is set to be fully charged in fast mode, and the charge duration is represented by (15):

$$T_c = \frac{E_i^{all} - E_i}{P_c^{fast}} \tag{15}$$

where P_c^{fast} represents the fast charging power.

2) WHEN THE DISTRIBUTION NETWORK FAILS

When the distribution network fails, the slow charging and fast charging behavior of EVs under the condition are shown in Fig. 2.

C. DISCHARGING BEHAVIOR

1) DISCHARGING PROBABILITY AND DISCHARGING ENERGY

If the electric vehicle is the "Part" type in parking place, there is a probability p_a that it is connected to the grid. When the distribution network fails and a V2G operation performed by electric vehicles is required, the electric vehicles connected to the grid will perform V2G operation if their battery state of charge satisfies (16):

$$SOC_i > S_y \tag{16}$$

where S_y represents the V2G discharging threshold. It is assumed that V2G operation calls up to 25% of battery power for a single electric vehicle.

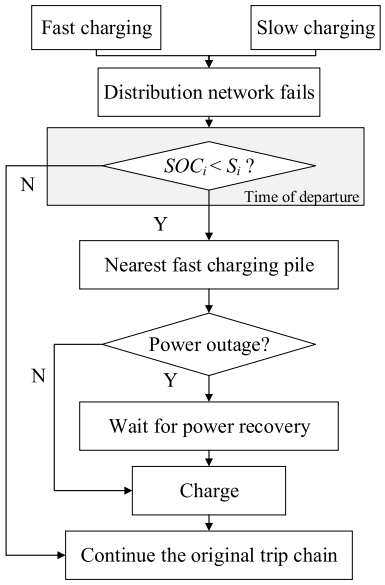

FIGURE 2. Slow charging and fast charging behavior of EVs.

2) THE EARLIEST DISCHARGING TIME AND DISCHARGING END TIME

The earliest discharging time of an electric vehicle is denoted as T_{DS}; the end time of discharging is denoted as T_{DE}; the start time of fault is denoted as T_{GS}; and the end time of fault is denoted as T_{GE}. There are three kinds of relationships among the four moments, as shown in Fig. 3.

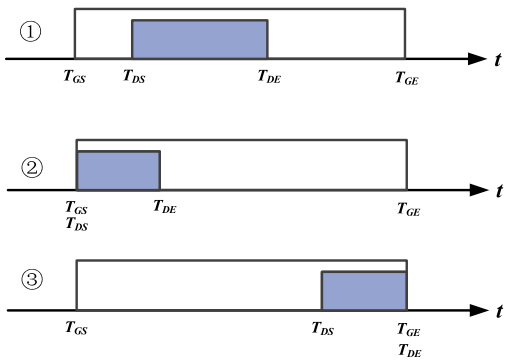

FIGURE 3. The earliest discharging start time and discharging end time.

Due to the actual scheduling, the electric vehicle may not keep discharging all the time during T_{DS} and T_{DE}. The discharging power is recorded as P_d. For each vehicle, the remaining battery power after V2G is:

$$E_i^{T_{DE}} = E_i^{T_{DS}} - \int_{T_{DS}}^{T_{DE}} P_d \cdot C(t)dt \tag{17}$$

where $C(t)$ is a 0-1 variable, where 1 means the electric vehicle is discharging, and 0 means remaining time.

IV. DISTRIBUTION NETWORK RELIABILITY ASSESSMENT

The temporal-spatial distribution and real-time SOC of electric vehicles are obtained above. Based on this, the reliability of the power system and the charging and discharging reliability of electric vehicles can be analyzed.

A. RELIABILITY PARAMETERS

Since electric vehicles have V2G capabilities, they are both power source and load. Their V2G and G2V have close relationship with their temporal-spatial characteristics, so it is necessary to consider this particularity and define some new parameters for the reliability of electric vehicles.

1) ELECTRIC VEHICLE RELIABILITY PARAMETERS

(1) Average Interruption Frequency of EV Charging Index (E_{AIFI}, times/year):

$$E_{AIFI} = \frac{\sum_{i=1}^{N} \lambda_i}{N \cdot Y} \tag{18}$$

where λ_i is the number of charge interruptions during the simulation time for electric vehicle i; N is the total amount of electric vehicles; Y is the number of simulation years.

(2) Average Interruption Duration of EV Charging Index (E_{AIDI}, hour/year):

$$E_{AIDI} = \frac{\sum_{i=1}^{N} t_i}{N \cdot Y} \tag{19}$$

where t_i is the total charging interruption time of the electric vehicle i within the simulation time.

(3) Average Extra Length for Charging (E_{AELC}, km/year)

$$E_{AELC} = \frac{\sum_{i=1}^{N} \Delta l_i}{N \cdot Y} \tag{20}$$

where Δl_i is the total distance of electric vehicle i to search for a new charging station due to a blackout when $SOC_i < S_i$ within the simulation time.

(4) Average Extra Time for Charging (E_{AETC}, min/year)

$$E_{AETC} = \frac{\sum_{i=1}^{N} \Delta t_i^E}{N \cdot Y} \tag{21}$$

where Δt_i^E is the total time of electric vehicle i to search for a new charging station due to a blackout when $SOC_i < S_i$ within the simulation time.

(5) Average Frequency of EV Participating in V2G (E_{AFPV}, time/year):

$$E_{AFPV} = \frac{\sum_{i=1}^{N} c_i}{N \cdot Y} \tag{22}$$

where c_i denotes the total number of times that electric vehicle i participated in V2G within the simulation time.

(6) Average Amount of Energy for EV Participating in V2G (E_{AEPV}, kWh/year):

$$E_{AEPV} = \frac{\sum_{i=1}^{N} e_i^a}{N \times Y} \tag{23}$$

where e_i^a represents the total energy provided by the electric vehicle i in V2G during the simulation time.

2) GRID SYSTEM RELIABILITY PARAMETERS

Since EVs are mobile and interruptible loads for the distribution network, the power outage has little impact on them when battery level are sufficient. Therefore, the system reliability index below refers to a conventional distribution network system that removes electric vehicles.

(1) System Average Interruption Frequency Index (S_{AIFI}, time/(household3·year)):

$$S_{AIFI} = \frac{\sum_{i=1}^{M} f_i}{M \cdot Y} \tag{24}$$

where f_i is the total number of power interruptions for user i within the simulation time, and M is the total number of household.

(2) System Average Interruption Duration Index (S_{AIDI}, min/(household·year)):

$$S_{AIDI} = \frac{\sum_{i=1}^{N} t_i^s}{M \cdot Y} \tag{25}$$

where t_i^s indicates the total duration of power outage of user i during simulation time.

(3) System Expected Energy Not Supplied (S_{EENS}, MWh/(household·year)):

$$S_{EENS} = \frac{\int_0^Y P_c(t)dt}{Y} \tag{26}$$

where $P_c(t)$ is the load curtailment of system at time t, $P_c(t)$ is 0 when the network is in the normal working condition.

B. ISLAND POWER SUPPLY MODEL

When a fault occurs in the distribution network, the total power generation and load satisfy the power balance:

$$\sum_{i=1}^{N_{dEV}} P_d^i(t) + \sum_{i=1}^{N_{dDG}} P_{DG}^i(t) \geq \sum_{i=1}^{N_L} L_i(t) \tag{27}$$

where N_{dEV} denotes the number of electric vehicles that can participate in V2G at time t. N_{dDG} is the number of distributed power sources that can generate electricity in isolated islands at time t. N_L indicates the number of load points in the island. $L_i(t)$ is the load of the i-th load point at time t. $P_d^i(t)$ is the discharging power of the i-th electric vehicle at time t. $P_{DG}^i(t)$ is the output of the i-th distributed power source at time t. The charging load of EV in the island is set as the lowest power supply level.

C. RELIABILITY ASSESSMENT BASED ON MONTE CARLO SIMULATION

1) WHEN THE DISTRIBUTION NETWORK IS OPERATING NORMALLY

According to the established model of temporal-spatial transition of electric vehicles, their travel and charging are simulated in a time-series manner. When the next activity begin, the simulation time advances directly to the start time of the activity. After completing the calculation of the first vehicle, the next vehicle is cycled until the last car on the day is calculated.

2) WHEN THE DISTRIBUTION NETWORK FAILS

For failures that do not cross days (Failure occurred at 0:00-24:00), a large simulation cycle is performed on a day-by-day basis and a small simulation cycle is performed on a single vehicle basis. The influence of the fault on the charging of the electric vehicle and V2G are taken into account. As shown in Fig. 4.

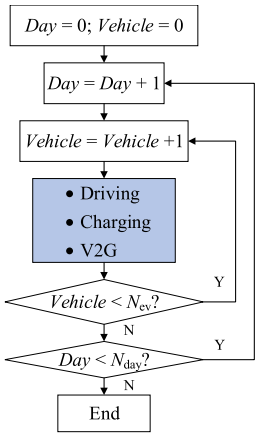

FIGURE 4. Fault time simulation flow chart.

For electric vehicle i that suffered a blackout at worksite K and satisfies the V2G conditions, its one-day timing event is shown in Fig. 5.

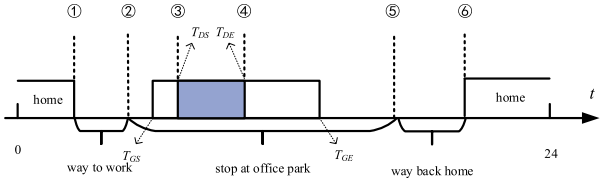

FIGURE 5. EV i timing diagram during the fault period.

where ① means starts from home; ② means arrives at the company; ③ means that there is a power outage at that location, and electric vehicle i starts to participate in V2G; ④ means that V2G ends due to satisfaction of constraints; ⑤ means leaves the company; ⑥ means returns home.

Because the simulation is based on a single vehicle cycle in the V2G process, there are actually multiple electric vehicles

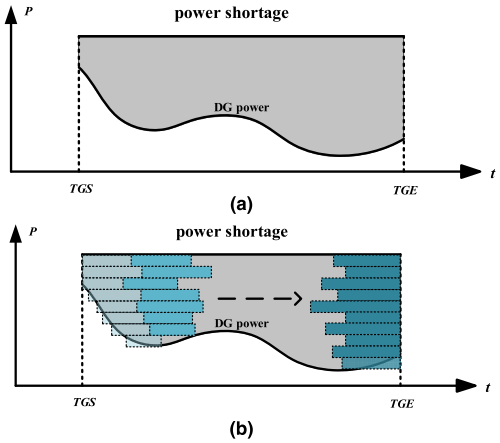

FIGURE 6. (a) Island power shortage. (b)"Post-fault settlement" V2G schematic.

supplying power to islands at the same time. We propose a method called "post-fault settlement" to calculate the participation of multiple electric vehicles participating in V2G, as shown in Fig. 6.

For electric vehicle i, the fault period is within the time interval of its parking, and the time interval that can participate in V2G is $T_{DS} - T_{DE}$. In the actual schedule, this interval can be moved to $T_{GS} - T_{GE}$ and only a part of the interval may be scheduled. During the simulation, the program only calculates the earliest V2G time and maximum discharging duration of electric vehicle i. For faulty node K, there are different numbers of electric vehicles in the $T_{GS} - T_{GE}$ period that can participate in V2G, and the V2G start time and maximum discharging duration of each electric vehicle are different. The grey part in Fig. 6(a) shows the power shortage except for the output of the distributed power in the island. This part needs electric vehicles to participate in V2G to supply.

After the end of the simulation of all electric vehicles, all electric vehicles that can participate in V2G in islands are sorted according to the earliest possible V2G time. The simulation first dispatches the top-ranking electric vehicle, and then the rear-ranked electric vehicle until they meet the load power shortage. The number of electric vehicles that are dispatched can be expressed as equation (28):

$$\begin{aligned} &\min\ N_{dEV} \\ &s.t.\ \sum_{i=1}^{N_{dEV}} P_d^i(t) + \sum_{i=1}^{N_{dDG}} P_{DG}^i(t) \geq \sum_{i=1}^{N_L} L_i(t) \\ &\quad \sum_{i=1}^{N_{dEV}-1} P_d^i(t) + \sum_{i=1}^{N_{dDG}} P_{DG}^i(t) < \sum_{i=1}^{N_L} L_i(t) \end{aligned} \tag{28}$$

where N_{dEV} is the number of electric vehicles. If the power shortage cannot be met, N_{dEV} is the maximum available number.

Fig. 6(b) is the schematic diagram of electric vehicles dispatching. Each square represents the time zone and discharging power of an electric vehicle participating in V2G. Light colors indicate electric vehicles that are dispatched first while dark colors indicate electric vehicles that are dispatched later. According to the energy consumed by each electric vehicles participating in V2G, the battery power will subtract the corresponding energy as equation (17). Finally, we calculate the reliability parameters for each node of the day. Since electric vehicles still have enough energy after participating in V2G, V2G will not affect the travel of electric vehicles on the day. Therefore, the simulation method results are consistent with the real-time updating results.

For failures that cross days, we increase the cycle period from one day to the number of days spanned by the fault, and calculate reliability parameters on the day when the fault ends.

V. NUMERICAL RESULTS

A. PARAMETER SETTINGS

Case studies are performed on an improved IEEE-RBTS Bus6 Test System to examine the performance of the proposed approach [22]. The system is shown in Fig. 7, including 1 section bus, 32 feeder sections, 26 nodes, 23 distribution transformers, 23 load points (LP1 to LP23), and 21 isolation switches.

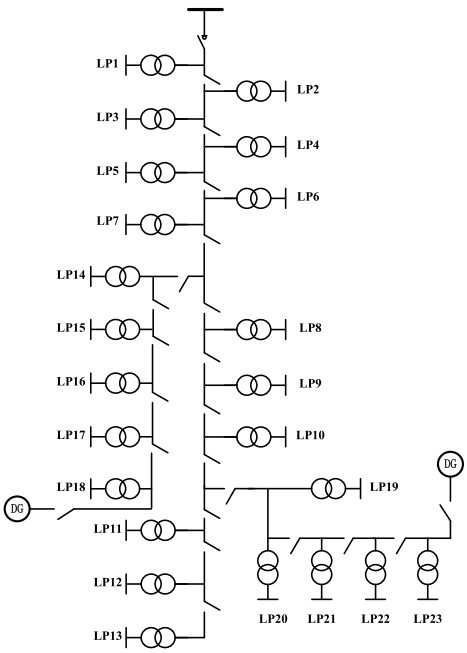

FIGURE 7. IEEE-RBTS bus6 test system.

This article assumes that the isolation switch is 100% successful each time. The distribution network is equipped with two distributed power supplies, each distributed power supply equipped with a total of 2010 kW wind power. Variations of wind speed can be represented by Weibull distributions.

Traffic network takes the main road in a typical city as an example, as shown in Fig. 8. It contains 17 nodes and 37 edges with colors on each side which represent its road grade.

TABLE 3. Quasi-dynamic path simulation results.

Period (h)	Actual path	Actual path time (h)	Shortest path time (h)
6-6.5	1-6-9-11-12	0.205	0.205
6.5-7	1-6-9-11-12	0.205	0.205
7-7.5	1-6-9-11-12	0.22	0.22
7.5-8	1-6-9-11-12	0.27	0.27
8-8.5	1-6-9-11-15-12	0.33	0.37
8.5-9	1-6-9-11-15-12	0.405	0.43
9-9.5	1-6-9-11-15-12	0.395	0.41
9.5-10	1-3-10-15-12	0.371	0.375

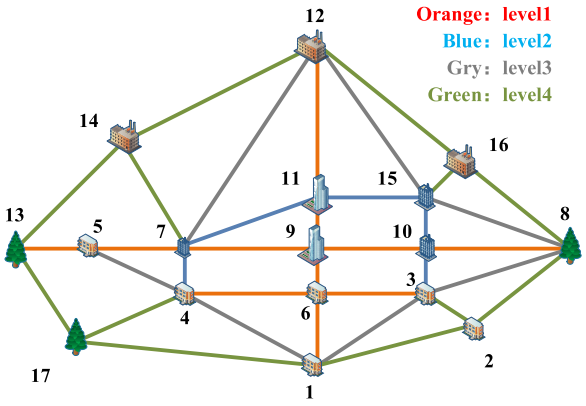

FIGURE 8. Traffic network.

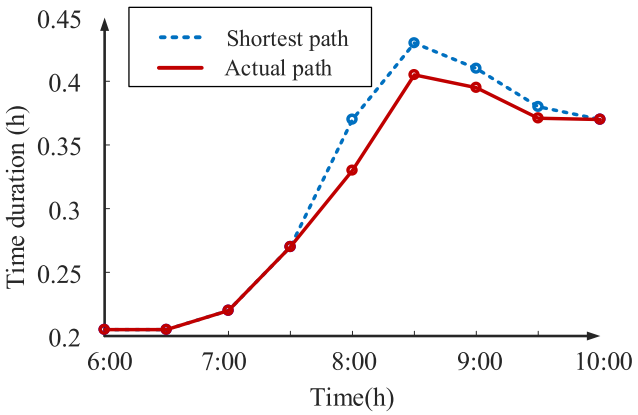

FIGURE 9. The time taken by the physical shortest distance and the actual path of the electric vehicle.

Among them, nodes 1-6 are residential areas (H), nodes 7, 8, 9, 10, 11, 12, 14, 15, and 16 are industrial and commercial areas (W), and nodes 8, 13 and 17 are entertainment shopping and leisure areas (SR/SE/O). The geographically coupled correspondence between traffic nodes and distribution network nodes is given in Annex.

Based on the population distribution of the main urban area of the city, the total travel OD matrix is obtained through the unconstrained gravity model [23]. The electric vehicle is based on Nissan LEFT EV with a battery capacity of 40kWh, fast charging power of 25kW, slow charging power of 6.6kW [24], and discharging power is set to 4.5kW. The SOC of all electric vehicles is set to 100% at the start of the simulation. The number of cars is to be 12,000. The number of OD layers in each trip is 48, and the simulation time is 400 years. The studies are performed on a PC with Intel Core i5 CPU 3.00 GHz and 6.00 GB RAM. The total CPU time consumption is 2.132×10^5 seconds. This paper assumes that each road network node is equipped with electric vehicle charging and discharging facilities.

B. QUASI-DYNAMIC PATH SIMULATION RESULTS

Taking *OD* 1 to 12 as an example, the path simulation in the morning is shown in Table 3. The time taken by the physical shortest distance and the actual path of the electric vehicle at different periods is shown in Fig. 9. The simulation results reveal that the shortest distance path at the non-working peak period (6:00-7.30 and 9:30-10.30) with relatively smooth traffic is also the shortest time path. The arrival of the peak hours of work (7:30-9:30) caused the shortest distance path to be congested, which increased the passage time. Electric vehicle would choose other roads with shorter travel time.

In addition, the changes of traffic flow in each section of a day were investigated, and the three sections, 2-3, 7-12 and 3-6, were taken as examples. The road traffic condition of three sections within 24 hours is shown in Fig. 10.

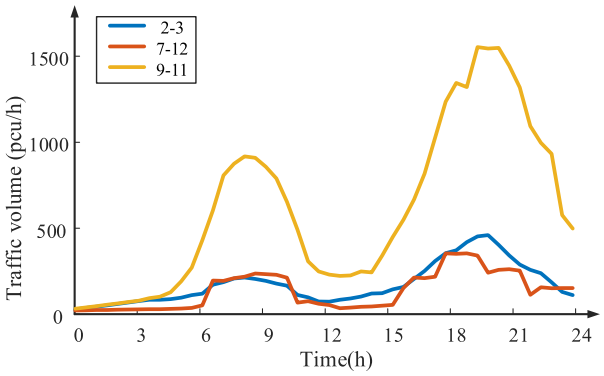

FIGURE 10. Road traffic condition.

As can be seen from the simulation results, the road network has two travel peaks every day, namely, going to work and going home, and the evening peak is higher than the morning peak, which is about 160% of the morning peak, and lasts longer. The morning peak lasts about 4 hours, and the evening peak lasts about 5 hours. The simulation results are consistent with the real urban congestion. It is shown that

the quasi-dynamic traffic flow simulation method proposed in this paper can simulate the dynamic traffic situation by using discrete method.

C. CHARGING AND DISCHARGING POWER OF ELECTRIC VEHICLE DURING FAULT PERIOD

As shown in Fig. 11, one day during the process of simulation of the distribution network nodes 18 (network node 1), front line fault due to power outage, switch action after the occurrence of fault movement, the node 18 and distributed power form supply island. As an emergency power supply, electric vehicles and distributed power supply to the island except electric vehicles.

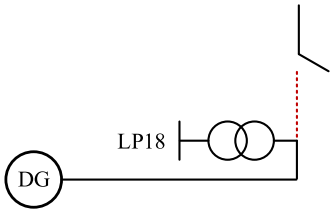

FIGURE 11. Fault circuit diagram.

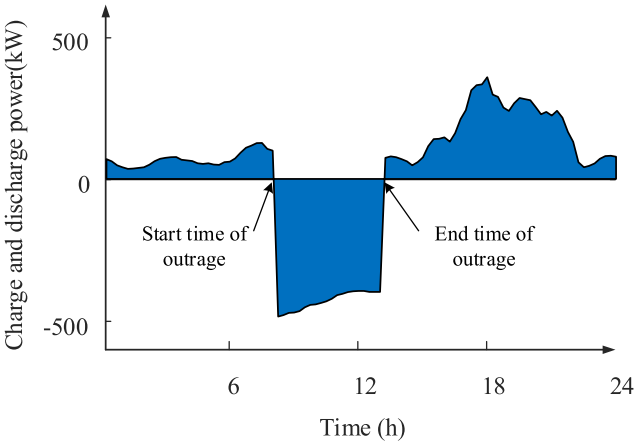

FIGURE 12. Charging and discharging load of electric vehicle.

In order to intuitive display, suppose nodes 18 is a constant load with 1000 kW (electric vehicle charging load is not concluded). The charging and discharging power distribution of electric vehicles at node 18 on that day is shown in Fig. 12, where positive value represents charging load and negative value represents discharging power. The fault starts at 8 AM, ends at 13 PM, which lasts for 5 hours. It can be seen from the figure that the charging power of EV at the same node is less than the discharging power, because the proportion of EV charging demand is small, a large proportion of EV can provide power to the distribution network, and most of EV are parked at that time. Output of electric vehicles and distributed power supply is shown in Fig.13. V2G and distributed power supply can fully meet the power load of island node 18.

D. IMPACT OF V2G TECHNOLOGY

When there are 6000 electric vehicles (40% penetration rate) in the power supply area, the chargeable probability is 0.9.

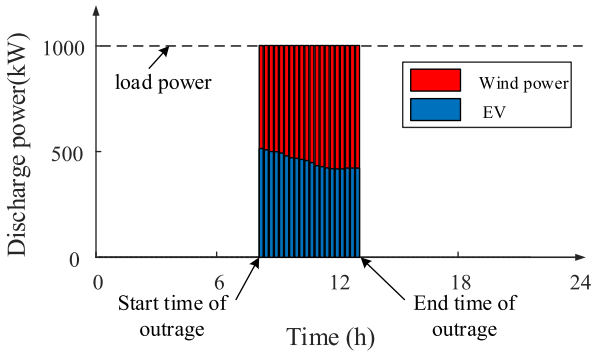

FIGURE 13. Electric vehicle V2G output and distributed power supply.

First, we consider a scenario that without V2G technology, all electric vehicles are only considered as grid loads. Second, scenario where all electric vehicles participate in V2G is considered. The system reliability of the two scenarios is shown in Table 4.

TABLE 4. Influence of V2G on reliability of distribution network.

V2G	S_{AIFI} (time·a^{-1})	S_{AIDI} (h·a^{-1})	S_{EENS} (MWh·a^{-1})
No	1.277	4.451	29.52
Yes	0.8364	3.341	22.14

It can be seen from Table 4 that in the case of V2G technology, S_{AIFI}, S_{AIDI} and S_{EENS} are all significantly reduced since the electric vehicles can supply power to the load as a backup power source during a fault. It shows that the backup power supply of electric vehicles has a strong capability in the distribution network. It indicates that EV, as a backup power source, has a strong power supply capacity in the distribution network. In practical operation, if the stored energy of EV is fully utilized, the power failure index value can be effectively reduced and the operation condition can be improved.

E. IMPACT OF ELECTRIC VEHICLE PENETRATION

At present, electric vehicles are being vigorously promoted around the world, but the penetration rate of electric vehicles is at a relatively low level. Therefore, it is necessary to study the impact of electric vehicle penetration on the reliability of electric vehicles as technology development and continue to deepen. Table 5 and Table 6 are simulation results of the reliability parameters of the distribution network and the electric vehicle, respectively. The S_{AIFI} and S_{AIDI} results are drawn in Fig. 14.

From the above results, it can be seen that for the distribution network system, the increase in the penetration rate of the electric vehicles actually enhances the capacity of the backup power supply of the distribution network, thus the three indexes of distribution network reliability increase. For electric vehicles, the reliability parameters increase with the rise of the penetration. From the trend of the two frequency reliability parameters of the grid and the electric vehicle,

TABLE 5. Influence of electric vehicle penetration rate on distribution network reliability.

EV Penetration	S_{AIFI} (time·a^{-1})	S_{AIDI} (h·a^{-1})	S_{EENS} (MWh·a^{-1})
0%	1.277	4.451	29.52
20%	1.011	3.674	26.31
40%	0.8364	3.341	22.14
60%	0.6236	2.510	19.79
80%	0.6211	2.239	18.69
100%	0.6024	2.126	18.23

TABLE 6. (a) Influence of electric vehicle penetration rate on electric vehicle reliability. (b) Influence of electric vehicle penetration rate on electric vehicle reliability.

(a)

EV Penetration	E_{AIFI} (time·a^{-1})	E_{AIDI} (h·a^{-1})	E_{AEPV} (kWh·a^{-1})
0%	/	/	/
20%	0.3471	2.276	2.026
40%	0.3462	2.267	2.018
60%	0.3458	2.264	2.016
80%	0.3455	2.263	2.016
100%	0.3454	2.263	2.015

(b)

EV Penetration	E_{AELC} (km·a^{-1})	E_{AETC} (min·a^{-1})	E_{AFPV} (time·a^{-1})
0%	/	/	/
20%	5.241	10.24	0.3369
40%	5.237	10.21	0.3367
60%	5.235	10.20	0.3365
80%	5.234	10.19	0.3365
100%	5.234	10.19	0.3365

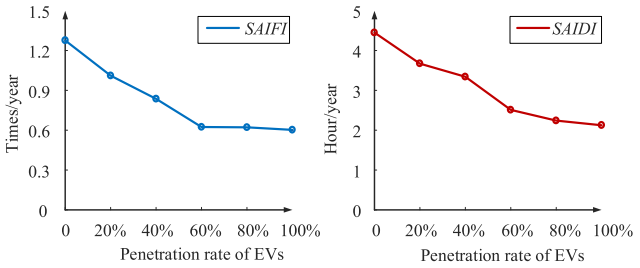

FIGURE 14. Penetration rate of electric vehicles.

the reliability parameters change caused by the increase in penetration from 20% to 60% is at a faster pace than the increase from 60% to 100%.

F. IMPACT OF DISCHARGE THRESHOLD

The V2G discharge threshold of an electric vehicle is equivalent to the activation condition of the standby power supply. The lower the threshold is, the easier it is to be activated, and the more significant the reliability of the distribution network is. Table 7 and Table 8 are simulation results of reliability parameters for distribution network and electric vehicle respectively.

It can be observed from the simulation results that the increase of the V2G discharge threshold has a significant improvement on the reliability of the grid. Especially when

TABLE 7. Influence of electric vehicle penetration rate on distribution network reliability.

Discharge threshold	S_{AIFI} (time·a^{-1})	S_{AIDI} (h·a^{-1})	S_{EENS} (MWh·a^{-1})
55%	0.5549	1.886	16.96
65%	0.6265	2.321	19.63
75%	0.8364	3.341	22.14
85%	0.9359	3.979	27.87

TABLE 8. (a) Influence of electric vehicle discharge threshold on reliability of electric vehicles. (b) Influence of electric vehicle discharge threshold on reliability of electric vehicles.

(a)

Discharge threshold	E_{AIFI} (time·a^{-1})	E_{AIDI} (h·a^{-1})	E_{AEPV} (kWh·a^{-1})
55%	0.3629	2.318	3.102
65%	0.3534	2.305	2.530
75%	0.3462	2.267	2.018
85%	0.3401	2.172	1.783

(b)

Discharge threshold	E_{AELC} (km·a^{-1})	E_{AETC} (min·a^{-1})	E_{AFPV} (time·a^{-1})
55%	5.412	10.77	0.5806
65%	5.289	10.36	0.4483
75%	5.237	10.21	0.3367
85%	5.213	9.854	0.2865

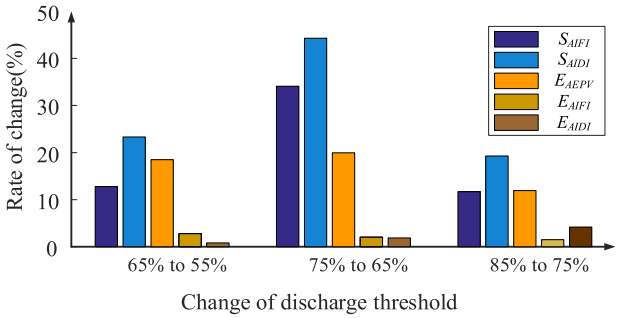

FIGURE 15. Reliability of the distribution network and electric vehicles.

S_y changes from 75% to 65%, the change rate of the three reliability parameters of the grid exceeds 30%. However, for the reliability of the electric vehicles, as shown in Fig. 15, the change of S_y mainly alters the energy of its participation in the discharge of V2G, and the influence on the charging reliability is not significant with respect to the reliability parameters of the distribution network.

G. IMPACT OF BATTERY CAPACITY

The battery capacity is currently the most important factor restricting the development of electric vehicles. For the charging reliability of electric vehicles, the increase in battery capacity makes the cruising range increase. Electric vehicles can choose to charge at a wider time scale, and the charging load of electric vehicles is distributed more evenly over time. For grid reliability, a larger battery capacity of EV means more energy that is callable. Table 9 and Table 10 are simulation results of reliability parameters for distribution network and electric vehicles, respectively.

TABLE 9. Influence of electric vehicle penetration rate on distribution network reliability.

Battery capacity kWh	S_{AIFI} (time·a^{-1})	S_{AIDI} (h·a^{-1})	S_{EENS} (MWh·a^{-1})
50	0.8373	3.382	25.25
60	0.8116	3.175	24.11
70	0.8030	3.109	23.75
80	0.8009	3.102	23.59

TABLE 10. (a) Influence of electric vehicle discharge threshold on reliability of electric vehicles. (b) Influence of electric vehicle discharge threshold on reliability of electric vehicles.

(a)

Battery capacity kWh	E_{AIFI} (time·a^{-1})	E_{AIDI} (h·a^{-1})	E_{AEPV} (kWh·a^{-1})
50	0.3462	2.267	2.018
60	0.3288	2.181	2.176
70	0.3217	2.016	2.305
80	0.3194	1.989	2.334

(b)

Battery capacity kWh	E_{AELC} (km·a^{-1})	E_{AETC} (min·a^{-1})	E_{AFPV} (time·a^{-1})
50	5.237	10.21	0.3367
60	5.097	9.928	0.4407
70	4.906	9.713	0.4684
80	4.905	9.707	0.4731

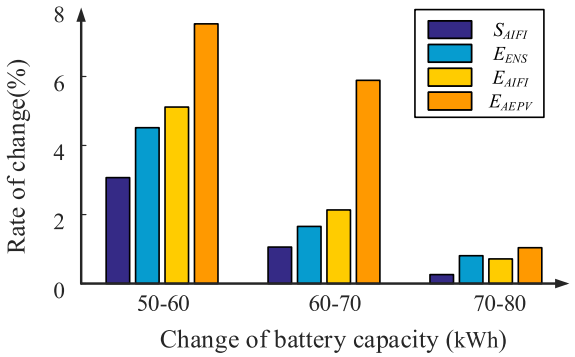

FIGURE 16. Changes in reliability parameters.

Changes in reliability parameters are shown in Fig. 16. It shows that the reliability parameters of the distribution network are obviously improved when the battery capacity of electric vehicles increases from 50 kWh to 60 kWh. When the battery capacity is high, the improvement of the reliability parameter is relatively limited. With the increase of the battery capacity, the charging reliability of electric vehicles is improved. This is because the increase in the battery capacity reduces the charging frequency, and the frequency of grid outages during the charge of electric vehicles.

H. ANALYSIS OF INFLUENCE OF ROAD IMPEDANCE ON RELIABILITY OF ELECTRIC VEHICLE AND DISTRIBUTION NETWORK

The emergence of electric vehicles strengthens the coupling relationship between road network and distribution network. From the perspective of road network, the increase in the number of cars on the road will aggravate the congestion and increase the road obstruction. On the other hand, the change of road resistance will directly affect the travel and charging and discharging behaviors of electric vehicles, and then affect the charging reliability of distribution network and electric vehicles. Road impedance depends on the number of cars in the road network. Therefore, this paper measures the road resistance by the total number of cars. Table 11 and 12 show the change of reliability index when the number of electric vehicles remains unchanged and the total number of vehicles keeps increasing.

TABLE 11. Influence of electric vehicle penetration rate on distribution network reliability.

EV ownership	S_{AIFI} (time·a^{-1})	S_{AIDI} (h·a^{-1})	S_{EENS} (MWh·a^{-1})
50	0.8364	3.341	22.14
60	0.8364	3.346	22.27
70	0.8365	3.352	22.39
80	0.8366	3.374	22.41

TABLE 12. (a) Influence of electric vehicle discharge threshold on reliability of electric vehicles. (b) Influence of electric vehicle discharge threshold on reliability of electric vehicles.

(a)

EV ownership	E_{AIFI} (time·a^{-1})	E_{AIDI} (h·a^{-1})	E_{AEPV} (kWh·a^{-1})
50	0.3462	2.267	2.018
60	0.3499	2.292	1.930
70	0.3621	2.354	1.898
80	0.3740	2.433	1.879

(b)

EV ownership	E_{AELC} (km·a^{-1})	E_{AETC} (min·a^{-1})	E_{AFPV} (time·a^{-1})
50	5.237	10.21	0.3367
60	5.322	10.31	0.3323
70	5.419	11.67	0.3283
80	5.573	11.84	0.3270

As can be seen from above results, with the increase of the number of cars in the road network, the congestion degree of the road network becomes worse. For electric cars, their charging reliability decreases gradually, and the number of times they can participate in V2G also decreases relatively. Compared with electric vehicles, the distribution network is less affected, and the number of power outages, duration of power outages and load loss indexes have a small decline.

VI. CONCLUSION

The random movements and the large amount of charging-discharging behaviors of electric vehicles generate huge calculations in reliability assessment. This paper makes some efforts to solve the problem of calculation efficiency and accuracy. Considering the influence of traffic congestion on path selection and computational efficiency, the static travel simulation is time-divided to realize the quasi-dynamic travel simulation. Temporal-spatial distribution and real-time SOC of electric vehicles are obtained, based on which, power system reliability and electric vehicle charging-discharging

reliability can be assessed. Moreover, a high efficiency Monte Carlo simulation method that improved the simulation time advancement is proposed to simulate the large amount of behaviors of electric vehicles. The results show that the quasi-dynamic travel simulation method simulates the influence of different congestion levels on path selection accurately. Fully considering the behaviors and quasi-dynamic path simulation of electric vehicles, the simulation takes only about 1.5 seconds for one day, which demonstrate the effectiveness of the proposed approach.

Analyses showed that the increase of the penetration rate of EVs, charging probability and the battery capacity are conducive to the reliability of the distribution network and electric vehicles charging. The reduction of the discharge threshold is beneficial to the improvement of the reliability of the distribution network, which is not conducive to the charging reliability of electric vehicles. When the number of electric vehicles is small or the battery capacity is low, increasing the number of EVs and battery capacity can effectively improve the distribution network and EVs' charging reliability. In addition, the charging and discharging load can be obtained through the proposed method, which can be used in EVs' charging load forecast.

APPENDIX

The geographically coupled correspondence between traffic nodes and distribution network nodes:

Road system node	Power system node
1	18
2	17
3	16
4	15
5	14
6	10
7	9
8	8
9	11
10	12
11	13
12	20
13	21
14	22
15	22
16	23
17	23

REFERENCES

[1] T. Mai, M. M. Hand, S. F. Baldwin, R. H. Wiser, G. L. Brinkman, P. Denholm, D. J. Arent, G. Porro, D. Sandor, D. J. Hostick, M. Milligan, E. A. DeMeo, and M. Bazilian, "Renewable electricity futures for the United States," *IEEE Trans. Sustain. Energy*, vol. 5, no. 2, pp. 372–378, Apr. 2014. doi: 10.1109/TSTE.2013.2290472.

[2] H. Pohl and M. Yarime, "Integrating innovation system and management concepts: The development of electric and hybrid electric vehicles in Japan," *Technol. Forecasting Social Change*, vol. 79, no. 8, pp. 1431–1446, Oct. 2012. doi: 10.1016/j.techfore.2012.04.012.

[3] L. C. Casals, E. Martinez-Laserna, B. A. García, and N. Nieto, "Sustainability analysis of the electric vehicle use in Europe for CO2 emissions reduction," *J. Cleaner Prod.*, vol. 127, pp. 425–437, Jul. 2016. doi: 10.1016/j.jclepro.2016.03.120.

[4] X. He, Y. Wu, S. Zhang, M. A. Tamor, T. J. Wallington, W. Shen, W. Han, L. Fu, and J. Hao, "Individual trip chain distributions for passenger cars: Implications for market acceptance of battery electric vehicles and energy consumption by plug-in hybrid electric vehicles," *Appl. Energy*, vol. 180, pp. 650–660, Oct. 2016. doi: 10.1016/j.apenergy.2016.08.021.

[5] Y. Sui, P. Yi, X. Liu, and T. Zhu, "Energy transport station deployment in electric vehicles energy internet," *IEEE Access*, vol. 7, pp. 97986–97995, 2019. doi: 10.1109/ACCESS.2019.2926408.

[6] F. R. Badal, P. Das, S. K. Sarker and S. K. Das, "A survey on control issues in renewable energy integration and microgrid," *Protection Control Mod. Power Syst.*, vol. 4, no. 4, pp. 87–113, 2019. doi: 10.1186/s41601-019-0122-8.

[7] P. Bangalore and L. Bertling, *Extension of Test System for Distribution System Reliability Analysis With Integration of Electric Vehicles in Distribution System*. Manchester, U.K.: ISGT Europe, 2011, pp. 1–7.

[8] C. X. Wu, C. Y. Chung, F. S. Wen, and D. Y. Du, "Reliability/cost evaluation with PEV and wind generation system," *IEEE Trans. Sustain. Energy*, vol. 5, no. 1, pp. 273–281, Jan. 2014. doi: 10.1109/TSTE.2013.2281515.

[9] B. Zhang, X. Yan, X. Xiao, H. Liu, and Y. Li, "The VSC parallel structure and control technology for the centralized V2G system," in *Proc. IEEE-ISIE*, Taiwan, China, May 2013, pp. 1–6.

[10] B. Rabah, J. Wang, M. Benbouzid, F. Khoucha, and M. Boudour, "Impact evaluation of large scale integration of electric vehicles on power grid," *Frontiers Energy*, to be published.

[11] H. Farzin, M. Moeini-Aghtaie, and M. Fotuhi-Firuzabad, "Reliability studies of distribution systems integrated with electric vehicles under battery-exchange mode," *IEEE Trans. Power Del.*, vol. 31, no. 6, pp. 2473–2482, Dec. 2016. doi: 10.1109/TPWRD.2015.2497219.

[12] M. R. Mozafar, M. H. Amini, and M. H. Moradi, "Innovative appraisement of smart grid operation considering large-scale integration of electric vehicles enabling V2G and G2V systems," *Electr. Power Syst. Res.*, vol. 154, pp. 245–256, Jan. 2018. doi: 10.1016/j.epsr.2017.08.024.

[13] W. Liu, M. Zhang, B. Zeng, L. Wu, and J. Zhang, "Analyzing the impacts of electric vehicle charging on distribution system reliability," in *Proc. ISGT Asia*, Tianjin, China, May 2012, pp. 1–6.

[14] N. Z. Xu and C. Y. Chung, "Reliability evaluation of distribution systems including vehicle-to-home and vehicle-to-grid," *IEEE Trans. Power Syst.*, vol. 31, no. 1, pp. 759–768, Jan. 2016. doi: 10.1109/TPWRS.2015.2396524.

[15] K. Hou, X. Xu, H. Jia, X. Yu, T. Jiang, K. Zhang, and B. Shu, "A reliability assessment approach for integrated transportation and electrical power systems incorporating electric vehicles," *IEEE Trans. Smart Grid*, vol. 9, no. 1, pp. 88–100, Jan. 2018. doi: 10.1109/TSG.2016.2545113.

[16] M. Carey, "Nonconvexity of the dynamic traffic assignment problem," *Transp. Res. B, Methodol.*, vol. 26, no. 2, pp. 127–133, Apr. 1992. doi: 10.1016/0191-2615(92)90003-F.

[17] *TransCAD Transportation Planning Software*. Accessed: Mar. 8, 2019. [Online]. Available: https://www.caliper.com/tcovu.htm

[18] J. Cong, L. Gao, and Z. Juan, "Improved algorithms for trip-chain estimation using massive student behaviour data from urban transit systems," *IET Intell. Transp. Syst.*, vol. 13, no. 3, pp. 435–442, Mar. 2019. doi: 10.1049/iet-its.2018.5183.

[19] 2009 National Household Travel Survey. U.S. Department of Transportation, Federal Highway Administration. New York, NY, USA. Accessed: Nov. 26, 2018. [Online]. Available: http://nhts.ornl.gov

[20] N. Zhou, X. Xiong, and Q. Wang, "Probability model and simulation method of electric vehicle charging load on distribution network," *Electr. Power Compon. Syst.*, vol. 42, pp. 879–888, Jul. 2014. doi: 10.1080/15325008.2014.903537.

[21] J. W. Lien, V. V. Mazalov, A. V. Melnik, and J. Zheng, "Wardrop equilibrium for networks with the BPR latency function," in *Proc. DOOR*, Vladivostok, Russia, 2016, pp. 37–49.

[22] R. Billinton and S. Jonnavithula, "A test system for teaching overall power system reliability assessment," *IEEE Trans. Power Syst.*, vol. 11, no. 4, pp. 1670–1676, Nov. 1996. doi: 10.1109/59.544626.

[23] J. Zhang and K. Liu, "A labeling link intensity algorithm in OD trip spatial distribution model," in *Proc. IEEE ITSC*, Washington, WA, USA, Oct. 2004, pp. 222–226.

[24] Nissan. *Nissan Leaf Range & Charging*. Accessed: May. 20, 2019. [Online]. Available: https://www.nissanusa.com/vehicles/electric-cars/leaf/range-charging.html

QIAN ZHANG (M'16) received the B.S., M.S., and Ph.D. degrees in electrical engineering from Chongqing University, Chongqing, China, in 2001, 2004, and 2009, respectively. In 2004, she joined Chongqing University, where she has been an Associate Professor with the Department of Electrical Engineering, since 2011. Her research interests include technologies of vehicle-to-gird, power system analysis and calculation, power market, and smart grid.

YI ZHU received the B.S. degree in electrical engineering from Chongqing University, Chongqing, China, in 2016, where he is currently pursuing the master's degree with the Department of Electrical Engineering. His research interests include technologies of vehicle-to-gird and power system reliability assessment.

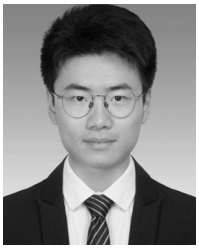

ZHONG WANG received the B.S. and M.S. degrees in electrical engineering from Chongqing University, Chongqing, China, in 2016 and 2019, respectively. He has joined State Grid Chengdu Power Supply Company. His main research interests include power system planning and power system reliability assessment.

YAOJIA SU received the B.S. degree from the School of Electrical Information, Wuhan Institute of Technology, China, in 2018. He is currently pursuing the M.S. degree with the Department of Electrical Engineering, Chongqing University. His current research interests include power market and blockchain.

CHUNYAN LI (M'16) received the B.S., M.S., and Ph.D. degrees in electrical engineering from Chongqing University, Chongqing, China, in 1998, 2001, and 2008, respectively. In 2003, she joined Chongqing University, where she has been an Associate Professor with the Department of Electrical Engineering, since 2008. Her research interests include demand response, power system analysis, and smart grid.